Journal of Crystal Growth 311 (2009) 2798–2801

Contents lists available at ScienceDirect

Journal of Crystal Growth

journal homepage: www.elsevier.com/locate/jcrysgro

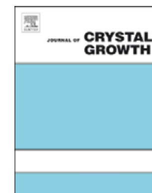

InN excitonic deformation potentials determined experimentally

B. Gil [a,*], M. Moret [a], O. Briot [a], S. Ruffenach [a], Ch. Giesen [b], M. Heuken [b], S. Rushworth [c], T. Leese [c], M. Succi [d]

[a] GES, UMR 5650 CNRS, CC074, Place Eugène Bataillon, Université Montpellier II, 34095 Montpellier, France
[b] AIXTRON AG, Kackertstr. 15-17, 52072 Aachen, Germany
[c] SAFC Hitech Limited, Power Road, Bromborough, Wirral, CH62 3QF, UK
[d] Saes Getters S.p.a., Viale Italia 77, 20020 Lainate (Mi), Italy

ARTICLE INFO

Available online 13 January 2009

PACS:
71.35.−y
61.10.Nz
81.15.Gh

Keywords:
A1. Excitonic deformation potential
B1. InN
A3. MOCVD

ABSTRACT

We report the experimental determination of the interband deformation potentials of indium nitride by combining both optical spectroscopy investigations and high-resolution X-ray measurements performed on a series of InN films grown by metal organic vapour-phase epitaxy. Our approach, which follows the one used for GaN by Shan et al. [Phys. Rev. B. 54 (1996) 13460], gives here for InN a_1=−7.66 eV, a_2=−2.59 eV, b_1=5.06 eV, and b_2=−2.53 eV.

© 2009 Elsevier B.V. All rights reserved.

1. Introduction

A tremendous activity has been dedicated to the comprehension of the growth mechanisms of indium nitride during the recent years. This renewal of interest has been correlated to the discovery of the low value (~650 meV) [1] of its fundamental band gap in contrast with the initial proposal at 2 eV [2]. The consequences of this are that nitrides, from AlN to InN, through GaN, a priori constitute an unique series of semiconductors with potential optoelectronic applications ranging from the ultra violet part of the electromagnetic spectrum to the infrared one. In addition, growing nitrides does not present environmental problems, and makes them candidates in terms of fulfilling the prescription of a sustainable growth society. It was also demonstrated that nitride alloys can be grown from AlN to GaN, from GaN to InN, from AlN to InN through the whole composition range [3]. Indium nitride-based quantum wells [4] were also realized as well as quantum dots [5], giving to this material a versatile range of applications.

In this paper, we determine experimentally the interband deformation potentials of indium nitride, which where only obtained from the theoretical point of view, so far, to the best of our knowledge. Their determination is the required passport if it is to envision the modeling of advanced devices, which is now in the range of short term aims, thanks to the progresses made concerning the p-doping of this material [6].

2. Experimental procedure

We proceed in the following way: a series of InN samples is grown under sufficiently different growth conditions which, we carefully check it by X-ray diffraction experiment, slightly changes the strain state of the nitride film without significantly modifying its residual doping. The photoluminescence energy of these samples is then plotted as a function of the values of c and a lattice parameters, that is to say as homothetic functions of the relevant components of the strain tensor e_{zz} and e_{yy}. Then, by comparing the numerical data with the standard predictions of the variation of the band structure of wurtzite nitrides with strain, a result of the invariants theory, we deduce the numerical values of the deformation potentials of indium nitride.

In order to determine the deformation potentials in InN, we need a series of good quality InN samples, with a spread of strain states, as large as possible. InN is a material very difficult to grow, due to the lack of lattice-matched substrate; it is in general grown under a high residual n-type. We grew our samples using metal organic vapour-phase epitaxy [7] in an AIXTRON AIX200/4RF-S reactor. Trimethylgallium and trimethylindium provided by SAFC Hitech Limited were used as group III element precursors, while ammonia was the nitrogen source. The purification of the carrier gases like H_2 and N_2, as well as NH_3 was ensured by a complete

*Corresponding author. Tel.: +33 467 143 924; fax: +33 467 143 760.
E-mail address: gil@ges.univ-montp2.fr (B. Gil).

0022-0248/$ - see front matter © 2009 Elsevier B.V. All rights reserved.
doi:10.1016/j.jcrysgro.2009.01.010

SAES setup of corresponding purifiers. InN was deposited either on sapphire (25% of lattice mismatch), or on GaN epilayers grown on sapphire (10% of lattice mismatch). Due to these huge lattice mismatches, the deposited InN is mostly relaxed, but a small residual strain still exists, which, previous investigations on GaN epilayers have shown it [8], is also influenced by the growth parameters (growth temperature, V/III molar ratio,...). Here, the growth temperature was varied in the 475–625 °C range, while the V/III molar ratio was changed from 5000 to 15,000. As we shall see later on, the spread of strain states is not so wide, and extremely careful measurements of the lattice parameters are required if it is to determine the strain state of the epilayer. The samples were characterized by Hall effect, in order to assess their residual carrier concentration. Values in the range $2\times10^{19}\,cm^{-3}$ were found for the residual electron concentrations, and in the precision of our experiment, the samples can be considered as similar in terms of doping. Hall effect measurements are sensitive to the electron accumulation layer usually formed at the air-exposed sample surface of InN [9]. A rather good estimate of the electron concentration can be derived from a fitting of the PL lineshape [10,11]. In the case of the electron concentration measured here, if $n=2\times10^{19}\,cm^{-3}$ corresponded to the bulk of the sample, the photoluminescence linewidth should be more than 250 meV [10,11]. In our case as shown in Fig. 1, the linewidth is sample independent and is about 70 meV that corresponds to an electron density approximately equal to $10^{18}\,cm^{-3}$. We can then consider that strain rather than doping [11] is the main effect contributing to the shift of the photoluminescence peak that we report for our samples. In all cases, the sapphire substrate is present in our structures. Thanks to its thickness, which is always two orders of magnitude larger than the thickness of the InN epilayers, and thanks to the high values of its elasticity coefficients we make the assumption that the sapphire substrates are unstrained. We will thus use the sapphire related diffraction peaks as a reference data to calibrate our measurements. A high-resolution X-ray diffraction Bruker D8 setup was used, the primary beam being passed through a Gobel mirror and a four-reflection Ge monochromator, in order to get a $CuK\alpha_1$ monochromatic intense beam. The *c*-lattice parameter of the substrate, optional GaN buffer layer and InN layer is then measured, in a large ω–2θ scan, from 14° to 22°, performed with a 0.001° step.

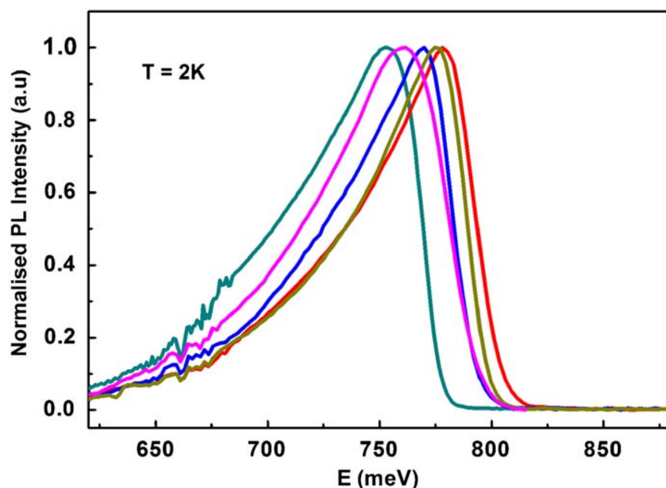

Fig. 1. Typical photoluminescence spectra taken on epilayers having different strain conditions, the corresponding *c* parameter ranging from 5.7060 to 5.7153 Å. An HeNe laser was used for excitation while detection was ensured by an extended InGaAs photodiode. From the Photoluminescence line shape, the residual n-type doping of the samples is about $10^{18}\,cm^{-3}$.

3. Results and discussion

The typical full-width of the (0 0 0 2) peak in our InN layers range from 600 to 1800 arcsec, depending on the growth conditions. The In or InN $(10\bar{1}1)$ peak, which is often observed in InN epilayers, is not present in most cases, or is very faint, and cannot induce any misinterpretation on the InN peak position, due to the relative "sharpness" of our peaks. Fig. 1 shows some typical photoluminescence spectra taken on epilayers having different values of *c*-lattice parameter.

The determination of the *a*-lattice parameter is more tricky, and epilayers usually exhibit larger in-plane default densities, which broaden the related X-ray diffraction patterns, compared to the growth direction. The relative width of the *a*-related peaks usually decreases the quality of the measurements and care must be exercised when recording such data. We have combined different approaches to extract the values of the InN *a*-parameter.

- First, grazing incidence X-ray diffraction (GID) experiments were performed. In our setup, the X-ray source can be rotated by 90° to enlarge the primary beam print on the sample in the GID configuration, to optimize the signal/noise ratio. As a matter of fact, an increase by a factor of 100 is obtained using this rotated setup. It should be noted here that InN, as well as GaN exhibits epitaxial relations such as the $(10\bar{1}0)$ planes of InN/GaN are aligned with $(11\bar{2}0)$ planes of the sapphire substrates. Here again, the sapphire peaks are used as a reference for the quantitative calibration of the measurements. Due to the grazing incidence, it happens in some samples, that the sapphire peaks are very weak. In these cases, the theoretical peak positions of the GaN buffer layer are calculated from the *c*-axis measurements, to serve as a reference.
- The measures are cross-checked by recording a reciprocal space map (RSM) of the region covering the $(10\bar{1}4)$ and $(11\bar{2}9)$ diffraction peaks of InN and sapphire, respectively. Once again, the sapphire substrate can be used as a reference to deduce the InN parameters. Such typical RSM is reported in Fig. 2. The RSM is plotted using the InN *h* and *l* parameters. In such coordinate system, the theoretical position of the substrate peak is $H=1.2878$ and $L=3.9530$ (here we have used the values $a=3.5390$ A and $c=5.7083$ A, as determined in Ref. [12], for InN.

Both measurements are in good agreement, and as it can be seen in Fig. 3(a), the *a*-lattice parameter of our samples decreases when the *c*-lattice parameter increases, which clearly indicates that the InN films experience a biaxial strain. The scattering indicates the difficulty to perform the quantitative determination of both *a* and *c* from high indices X-ray patterns. The photoluminescence energy also increases linearly with increasing *c* as can be seen in Fig. 3(b).

In order to determine the deformation potentials, one needs some information concerning the valence band physics in indium nitride. Due to the still important residual electron densities in indium nitride, nobody has been able so far to detect in a reflectivity experiment, the signature of exciton polariton at the energy position of the A, B, and C excitons typical of wurtzite semiconductors. Fortunately, Rüdiger Goldhahn et al. [13] have performed ellipsometry measurements on *c*-plane grown and polarized ellipsometry measurements on *a*-plane grown InN films. They unambiguously proposed the valence band ordering to be the natural Γ_9, Γ_7, Γ_7 ordering with a crystal field splitting parameter of 20–25 meV. Therefore, our photoluminescence involves recombination of electrons in quantum states sitting

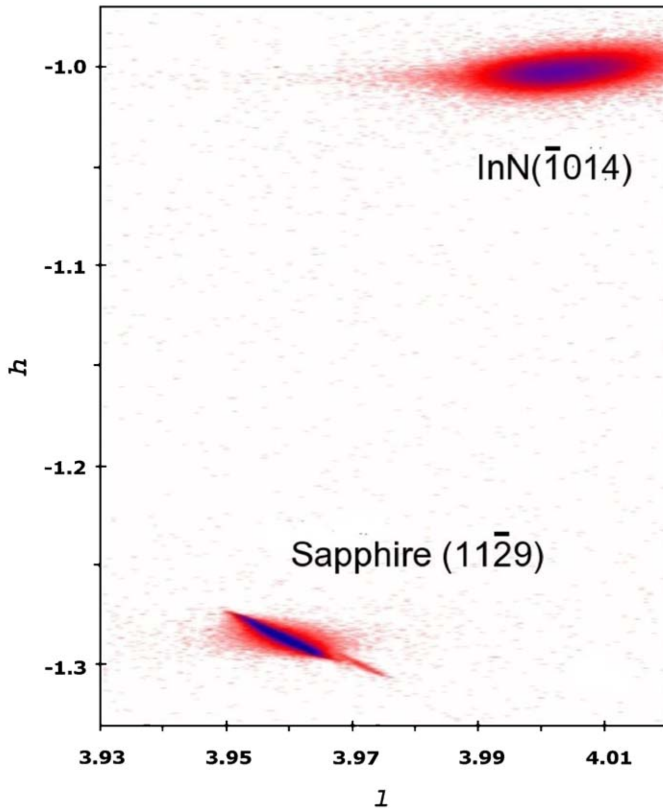

Fig. 2. Reciprocal space map (RSM) of the region covering the $(10\bar{1}4)$ and $(11\bar{2}9)$ diffraction peaks of InN and sapphire, respectively.

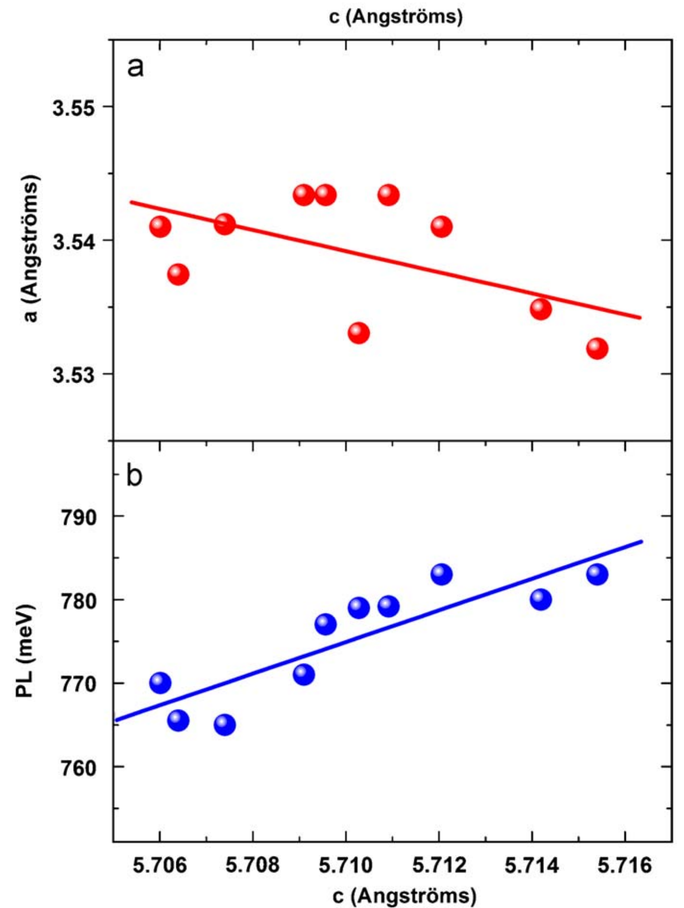

Fig. 3. The evolution of the a-lattice parameter (a) and the photoluminescence energy (b) of our samples, versus the c-lattice parameter. The sign and magnitude of the slope in (a) both indicate that the InN films experience a biaxial strain.

from the bottom of the conduction band up to the Fermi energy (this gives most of the contribution to the 70 meV linewidth) with a Γ_9 hole at low temperature. The photoluminescence feature shifts like the A line when the strain varies in our samples. We have not measured any in-plane anisotropy of our photoluminescence spectra. Therefore, by using group theory arguments we conclude that the wurtzite symmetry is kept by epitaxial growth. The residual strain field is either of pure hydrostatic kind or pure isotropic biaxial kind in the (0 0 0 1) growth plane [14].

$$E_A = E_A(0) + a_1 e_{zz} + a_2(e_{xx} + e_{yy}) + b_1 e_{zz} + b_2(e_{xx} + e_{yy}) \quad (1)$$

Deformation potentials a_1 and a_2 account for the average variation of the band gap, b_1 and b_2 account for the strain-induced variation of the crystal-field splitting parameter, e_{xx}, e_{yy} and e_{zz} are the components of the strain tensor. The quasi-cubic approximation [15] correlates some of these deformation potentials together. It states that the crystal field splitting only depends on the c/a ratio and would remain equal to zero upon application of an hydrostatic pressure, if the wurtzite nitride compound would behave like a cubic crystal (e_{xx}=e_{yy}=e_{zz}). This gives a first relation: $b_1 \approx -2b_2$. A second relation can be obtained by stating the quasi-equivalence of a cubic crystal that experiences a trigonal strain in the (1 1 1) plane and a biaxial strain experienced by the wurtzite crystal in its (0 0 0 1) basal plane. This gives our second relation: $a_1 - a_2 + b_1 = 0$. This has been extensively used for GaN [16–20] and we will applicate it for InN here. It is believed to overestimate a_2 and b_1 [21].

Thanks to the lack of in-plane optical anisotropy, a correlation exists between the components of the strain tensor

$$e_{xx} = e_{yy} = \frac{a - a_0}{a_0} = \kappa e_{zz} = \kappa \frac{c - c_0}{c_0} \quad (2)$$

$\kappa = -C_{33}/2C_{13}$ for an isotropic biaxial strain applied in the (0 0 0 1) growth plane and $\kappa_{hydro} = C_{33} - C_{13}/C_{11} + C_{12} - 2C_{13}$ when an hydrostatic pressure is applied to the crystal.

Eq. (1) is rewritten as

$$E_A = E_A(0) + [(a_1 + b_1) + 2\kappa(a_2 + b_2)]e_{zz} \quad (3)$$

The gradient the photoluminescence energy with the c-lattice parameter of InN is

$$\left(\frac{\partial E_A}{\partial c}\right) = \frac{(a_1 + b_1) + 2\kappa(a_2 + b_2)}{c_0} \quad (4)$$

This gives an experimental correlation between the values of the deformation potentials:

$$a_1 + 2\kappa a_2 + b_1 + 2\kappa b_2 = c_0 \left(\frac{\partial E_A}{\partial c}\right) \quad (5)$$

As seen at the top of Fig. 3(b), the experimental value of $\partial E_A/\partial c$=17 eV nm^{-1}. Values of $\partial E/\partial c$ measured for GaN films under weak biaxial compression [16] are 4.2 eV nm^{-1} for A and B excitons and 7.2 eV nm^{-1} for C excitons, whilst measured values of $\partial E/\partial a$ given in the same paper are—30 eV nm^{-1} and for A and B excitons and -52 eV nm^{-1} for C excitons.

A fourth equation is required to solve our system, which is obtained from hydrostatic pressure experiments available in the literature. The most recent experimental values of the pressure dependence of the band gap of InN are -30 meV/GPa [22] (compressions are negative quantities) in close agreement with

Table 1
Values of the excitonic deformation potentials in case of the GaN and InN semiconductors.

	a_1 (eV)	a_2 (eV)	b_1 (eV)	b_2 (eV)	Refs.
GaN (exp.)	−6.5	−11.8	−5.3	2.7	[16]
GaN (exp.)	−5.32	−10.23	−4.91	2.46	[17]
GaN (exp.)	−9.6	−8.2	1.9	−1.0	[18]
GaN (exp.)	−3.1	−11.2	−8.2	4.1	[19]
GaN (theory)	−4.09	−8.87	−7.02	3.65	[21]
InN (theory)	−3.5	−11.7	8.2	−4.1	[27]
InN (theory)	−4.05	−6.67	4.92	−1.79	[28]
InN (exp)	−7.66	−2.59	5.06	−2.53	This work

theoretical computations [19,21,23–25]. We take an average value of −30 meV/GPa here. Eq. (3) is therefore rewritten as a function of the pressure P [15]:

$$E_A = E_A(0) + [(a_1 + b_1) + 2\kappa(a_2 + b_2)]\frac{C_{11} + C_{12} - 2C_{13}}{(C_{11} + C_{12})C_{33} - 2C_{13}^2}P \qquad (6)$$

giving the fourth equation of the system of four unknowns

$$a_1 + 2\kappa_{\text{hydro}}a_2 + b_1 + 2\kappa_{\text{hydro}}b_2 = \frac{(C_{11} + C_{12})C_{33} - 2C_{13}^2}{C_{11} + C_{12} - 2C_{13}}\frac{\partial E_A}{\partial P} = \varpi\frac{\partial E_A}{\partial P} \qquad (7)$$

After some light algebra one obtains

$$\begin{cases} a_1 = -\dfrac{2\kappa_{\text{hydro}} + 2}{2\kappa_{\text{hydro}} - 2\kappa}c\dfrac{\partial E}{\partial c} + \dfrac{2\kappa + 2}{2\kappa_{\text{hydro}} - 2\kappa}\varpi\dfrac{\partial E}{\partial P} \\ a_2 = \dfrac{2\kappa_{\text{hydro}}}{2\kappa_{\text{hydro}} - 2\kappa}c\dfrac{\partial E}{\partial c} - \dfrac{2\kappa}{2\kappa_{\text{hydro}} - 2\kappa}\varpi\dfrac{\partial E}{\partial P} \\ b_1 = 2\dfrac{2\kappa_{\text{hydro}} + 1}{2\kappa_{\text{hydro}} - 2\kappa}c\dfrac{\partial E}{\partial c} - 2\dfrac{2\kappa + 1}{2\kappa_{\text{hydro}} - 2\kappa}\varpi\dfrac{\partial E}{\partial P} \\ b_2 = -\dfrac{2\kappa_{\text{hydro}} + 1}{2\kappa_{\text{hydro}} - 2\kappa}c\dfrac{\partial E}{\partial c} + \dfrac{2\kappa + 1}{2\kappa_{\text{hydro}} - 2\kappa}\varpi\dfrac{\partial E}{\partial P} \end{cases} \qquad (8)$$

Numerical calculations have been done using as stiffness coefficients in the following values: C_{11}=223 GPa, C_{12}=115 GPa, C_{13}=92 GPa, and C_{33}=224 GPa [26]. The values of the InN lattice parameters were taken from recent powder diffraction experiments: c_0=0.57083 nm and a_0=0.3539 nm [12].

The values we obtain are: a_1=−7.66 eV, a_2=−2.59 eV, b_1=5.06 eV, and b_2=−2.53 eV. They are the first experimental values of the electronic deformation potentials in indium nitride. For the sake of the comparison, we have given in Table 1 a series of experimental and theoretical values measured on GaN films and computed theoretically. As it can be seen, neither this measurement, nor this calculation, are trivial. This statement also holds in the case of indium nitride.

4. Conclusion

In conclusion, we have reported the first measurement of four of the six electronic deformation potentials of indium nitride by combining optical spectroscopy and high-resolution X-ray diffraction experiments in grazing incidence conditions and in the ω–2θ scan configurations. The InN deformation potentials values obtained are: a_1=−7.66 eV, a_2=−2.59 eV, b_1=5.06 eV, and b_2=−2.53 eV.

Acknowledgements

This work was supported by the European Commission under by Sixth Framework Program (STREP project "INDOT", Contract no. NMP4-CT-2005-016956).

References

[1] V.Yu. Davydov, A.A. Klochikhin, V.V. Emtsev, S.V. Ivanov, V.V. Vekshin, F. Bechstedt, J. Furthmuller, H. Harima, A.V. Mudryi, A. Hashimoto, A. Yamamoto, J. Aderhold, J. Graul, E.E. Haller, Phys. Status Solidi (b) R4 (2002) 330;
W. Shan, W. Walukiewicz, E.E. Haller, B.D. Little, J.J. Song, M.D. McCluskey, N.M. Johnson, Z.C. Feng, M. Schurman, R.A. Stall, J. Appl. Phys. 84 (1998) 4452.
[2] T.L. Tansley, C.P. Foley, J. Appl. Phys. 59 (1986) 3241.
[3] H. Morkoc, Handbook of Nitride Semiconductors and Devices, Materials Properties, Physics and Growth, vol. 1, Wiley-VCH, Berlin, 2008.
[4] M. Kurouchi, H. Naoi, T. Araki, T. Miyajima, Y. Nanishi, Jpn. J. Appl. Phys. 44 (2005) L230;
T. Ohashi, P. Holmstrom, A. Kikuchi, K. Kishino, Appl. Phys. Lett. 89 (2006) 041907;
S.B. Che, T. Mizuno, X.Q. Wang, Y. Ishitani, A. Yoshikawa, J. Appl. Phys. 102 (2007) 083539.
[5] S. Ruffenach, O. Briot, M. Moret, B. Gil, Appl. Phys Lett. 90 (2007) 153102.
[6] X. Wang, S.B. Che, Y. Ishitani, A. Yoshikawa, Appl. Phys. Lett. 91 (2007) 242111 and References therein.
[7] B. Maleyre, S. Ruffenach, O. Briot, B. Gil, A. Van der Lee, Superlattices Microstruct. 36 (2004) 517.
[8] B. Gil, O. Briot, Phys. Rev. B 55 (1997) 2530.
[9] J. Wu, W. Walukiewicz, K.M. Yu, J.W. Ager III, E.E. Haller, H. Lu, W.J. Schaff, Appl. Phys. Lett. 80 (2002) 4741.
[10] L. Colakerol, T.D. Veal, H.-K. Jeong, L. Plucinski, A. DeMasi, T. Learmonth, P.-A. Glans, S. Wang, Y. Zhang, L.F.J. Piper, P.H. Jefferson, A. Fedorov, T.-C. Chen, T.D. Moustakas, C.F. McConville, Kevin E. Smith, Phys. Rev. Lett. 97 (2006) 237601.
[11] E.O. Kane, Phys. Rev. 131 (1963) 79.
[12] B. Maleyre, S. Ruffenach, O. Briot, B. Gil, A. Van der Lee, Superlattices Microstruct. 36 (2004) 527.
[13] R. Goldhahn, A.T. Winzer, V. Cimalla, O. Ambacher, C. Cobet, W. Richter, N. Esser, J. Furthmüller, F. Bechstedt, H. Lu, W.J. Schaff, Superlattices Microstruct. 36 (2004) 591.
[14] B. Gil, O. Briot, R.L. Aulombard, Phys. Rev. B 52 (1995) R17028.
[15] G.E. Pikus, L.G. Bir, Symmetry and Strain-Induced Effects Semiconductors, Wiley, New York, 1994.
[16] W. Shan, R.J. Haunstein, A.J. Fischer, J.J. Song, W.G. Perry, M.D. Bremser, R.F. Davis, B. Goldenberg, Phys. Rev. B. 54 (1996) 13460.
[17] B. Gil, A. Alemu, Phys. Rev. B 56 (1997) 12446.
[18] H.Y. Peng, M.D. McCluskey, Y.M. Gupta, M. Kneissl, N.M. Johnson, Phys. Rev. B 71 (2005) 115207.
[19] S. Ghosh, P. Waltereit, O. Brandt, H.T. Grahn, K.H. Ploog, Phys. Rev. B 65 (2002) 075202.
[20] K. Kim, W.R.L. Lambrecht, B. Segall, Phys. Rev. B 53 (1996) 16310.
[21] M. Wagner, F. Bechstedt, Phys. Status Solidi (b) 234 (2002) 965.
[22] S.X. Li, J. Wu, E.E. Heller, W. Waluckiewicz, W. Shan, H. Lu, W.J. Schaff, Appl. Phys. Lett. 83 (2003) 4963 (and References therein).
[23] A. Kaminska, G. Fransen, T. Suski, I. Gorczyca, N.E. Christensen, A. Svane, A. Suchocki, H. Lu, W.J. Schaff, E. Dimackis, A. Georgakilas, Phys. Rev. B. 76 (2007) 075203.
[24] A. Janotti, D. Seguev, C.G. Van de Walle, Phys. Rev. B. 74 (2007) 045202-1.
[25] A. Janotti, C.G. Van de Walle, Phys. Rev. B. 75 (2007) 121201-1.
[26] A.F. Wright, A. Girndt, F. Janke, S.W. Koch, Mater. Res. Soc. Symp. Proc. 468 (1997) 487.
[27] J. Battacharyya, S. Gosh, Phys. Status Solidi (a) 204 (2007) 439.
[28] S.P. Lepkowski, J.A. Majewski, G. Jurczak, Phys. Rev. B. 72 (2007) 245201.